Rapid and extensive membrane reorganization by dendritic cells following exposure to bacteria revealed by high-resolution imaging

Russell D. Salter,*,[1] Renee J. Tuma-Warrino,* Paul Q. Hu,* and Simon C. Watkins*,†

*Departments of *Immunology and †Cell Biology and Physiology, University of Pittsburgh School of Medicine, Pennsylvania*

Abstract: Using live cell imaging, we demonstrate that immature dendritic cells (DC) derived from human peripheral blood monocytes undergo pronounced morphologic changes in vitro within minutes of exposure to unopsonized *Escherichia coli*, developing extensive membrane veils that efficiently capture additional bacteria. Internalization does not occur in the veils, but instead, bacteria are transported to the central region of the cell, where they sink directly into the plasma membrane. In contrast, exposure to polystyrene beads does not induce notable changes in cell morphology, and DC do not efficiently capture beads when introduced alone or mixed with bacteria. Long dendritic processes were also visualized in some cells that allowed capture of clumps of bacteria at a distance of more than 100 μm. These results demonstrate that immature DC can distinguish between inert particles and bacteria and alter their shape and phagocytic capacity in response to the latter. *J. Leukoc. Biol.* 75: 240–243; 2004.

Key Words: E. coli · *green fluorescent protein* · *phagocytosis*

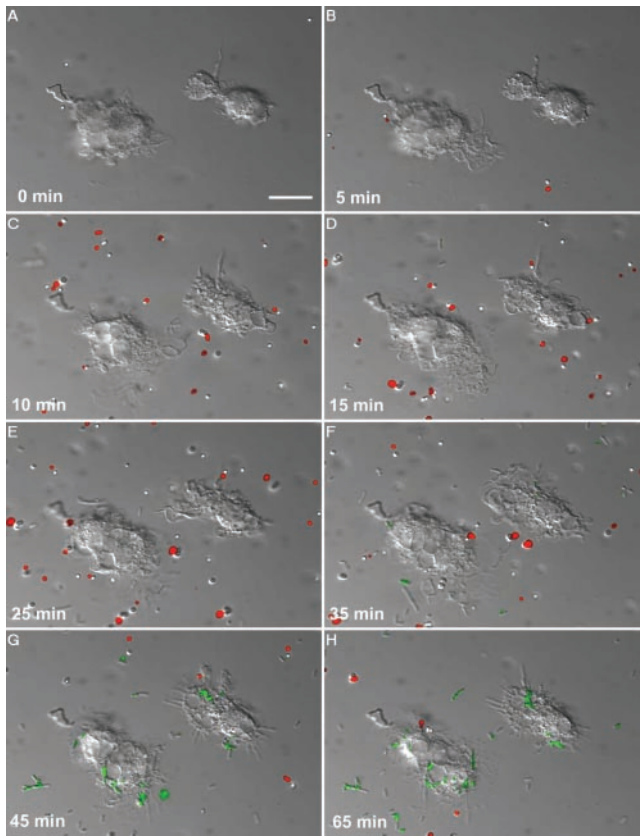

Fig. 1. Uptake of live enhanced green fluorescent protein (EGFP) expressing *Escherichia coli* (BL21 strain) by human monocyte-derived DC. DC were generated by culturing purified monocytes in GM-CSF and IL-4 for 5 days in tissue-culture flasks before plating onto collagen-coated coverslips. After overnight culture to allow for cell adhesion, coverslips were loaded into a closed live-cell imaging chamber, and six stage positions were selected to include representative cells. Fluorescent microspheres were then added to the culture via an airlock, and medium was washed through the chamber using a pump, delivering a flow rate of 1 ml/h. Images were collected as soon as beads were visualized within the cell chamber at 1-min intervals, and differential interference contrast, green, and red channels were collected for the duration of the experiment. Thirty minutes after addition of beads, EGFP-expressing *E. coli* were introduced via the airlock. The supplemental movies available at http://www.cbi.pitt.edu/movies/leuk.html represent the complete dataset from which these images were selected. White bar, 25 μm. The data shown are representative of three independent experiments using different preparations of DC, each with multiple stage positions analyzed.

Many forms of antigen can be internalized by immature or antigen-capturing dendritic cells (DC), which then can mature into antigen-presenting DC that efficiently stimulate T cell responses. Antigen uptake occurs by multiple mechanisms, including phagocytosis, macropinocytosis, and receptor-mediated endocytosis, via a number of receptors also expressed on macrophages and appears to be relatively nonselective, a feature that is important to allow for presentation of a wide array of exogenous antigens (reviewed in ref. [1]). DC can internalize a variety of particulates, including inert beads, iron oxide particles, apoptotic cells, bacteria, and yeast particles, and each has been used experimentally to deliver antigens for processing and presentation [2–6]. The relative efficiency of uptake of the different particulates has not been carefully compared, and there is little information to date regarding selectivity of the uptake process. We hypothesized that inert particles might differ from complex structures such as bacteria in the mechanism of uptake and subsequent effect on the cell.

[1] Correspondence: E1052 BST, 200 Lothrop Street, University of Pittsburgh School of Medicine, Pittsburgh, PA 15213. E-mail: rds@pitt.edu

Received July 21, 2003; revised October 10, 2003; accepted October 23, 2003; doi: 10.1189/jlb.0703339.

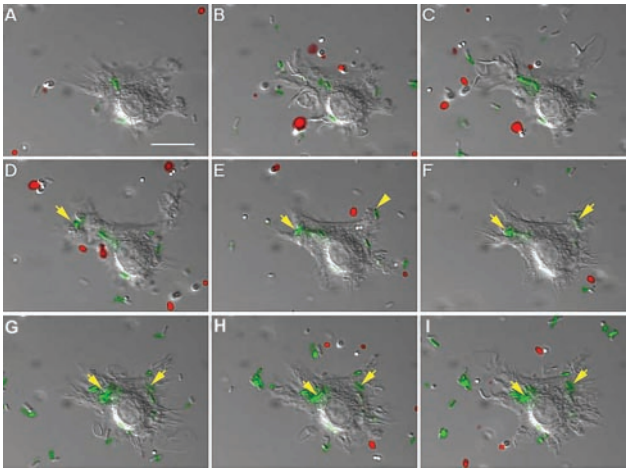

Fig. 2. Extension of pseudopods, which capture bacteria, but not beads flowing past the cell. Images were obtained during the same experiment shown in Figure 1 at a different stage position. Selected frames from a 14-min period are shown to exemplify major changes in cell morphology or particle/bacteria uptake, and the complete dataset is represented in a supplemental movie at http://www.cbi.pitt.edu/movies/leuk.html. Yellow arrows, Bacteria that are retracted toward the center of the cell. White bar, 25 μm.

To address this and obtain a detailed picture of particle uptake by DC, we have used high-resolution, live-cell imaging analysis. DC were obtained by culturing human monocytes for 5 days in medium containing granulocyte macrophage-colony stimulating factor (GM-CSF) and interleukin (IL)-4, as described [7]. These cells have an immature phenotype characterized by low expression of class I and class II major histocompatibility complex and little or no CD80, CD83, and CD86, as reported by others and us [7–10]. They are highly active at internalizing soluble ligands by macropinocytosis or by mannose receptor [8]. Following exposure to lipopolysaccharide or other compounds that stimulate maturation, maturational markers increase, and endocytic capacity is lost [8]. Detailed phenotypic analyses by flow cytometry were used to characterize them as DC lacking CD14, CD64, and CD68, all of which are present on cultured macrophages (ref. [7] and unpublished results).

Cells were grown on collagen-coated coverslips, which were placed in a continuous flow chamber system. Images were obtained using a Nikon Eclipse 2000E (Nikon Inc., Melville, NY), equipped with a water-cooled Hamamatsu Orca 2 ER camera (Hamamatsu, Tokyo, Japan) and a 60× 1.45NA plan apochromat objective. The software used was Simple PCI (Compix Inc., Cranberry, PA). Images were collected at multiple-stage positions at 1-min intervals. In **Figure 1**, time-lapse images are shown of experiments in which a single bolus of red polystyrene microspheres (FluoSpheres® F-8851, Molecular Probes, Eugene, OR) was injected into the closed chamber system via an airlock, and images were collected at multiple-stage positions at 1-min intervals as soon as beads

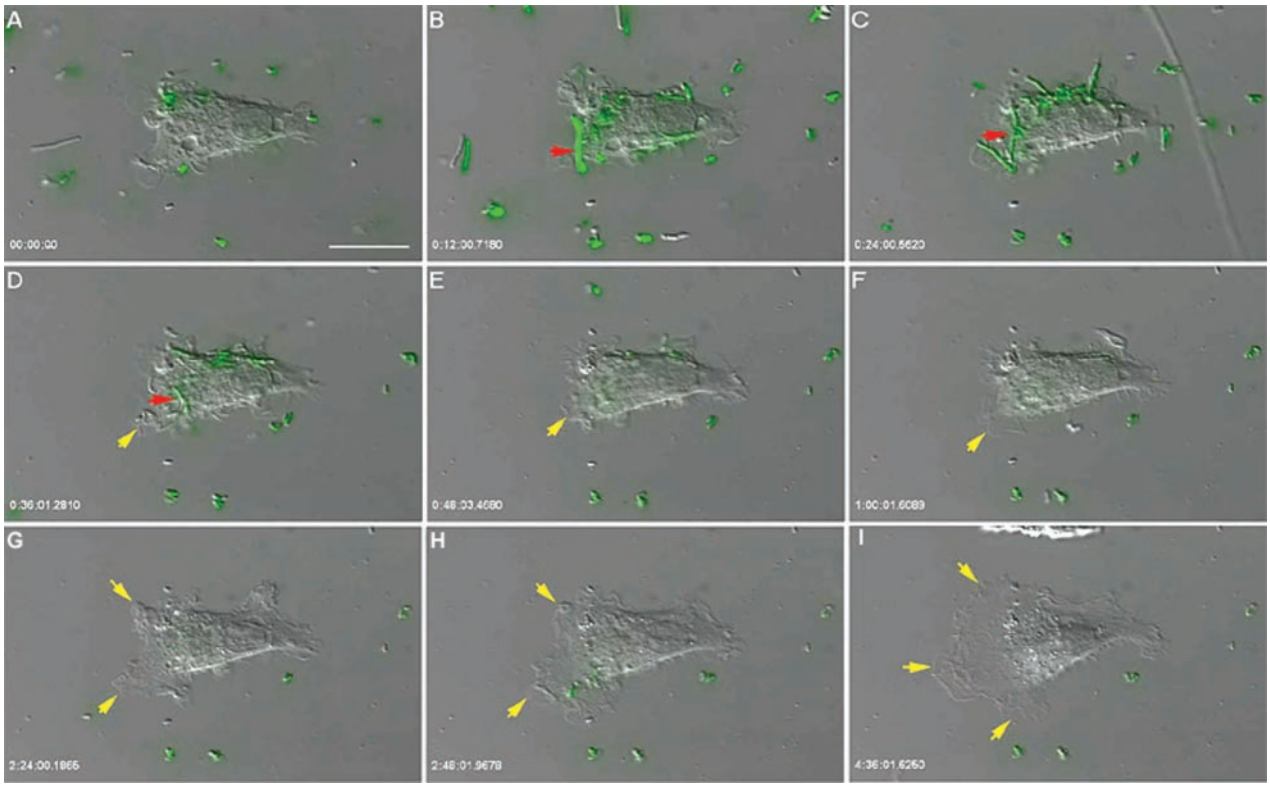

Fig. 3. Morphologic changes in DC following exposure to EGFP-expressing *E. coli*. DC were analyzed as in Figure 1, except that only *E. coli* were added. Images were collected as soon as bacteria were visulaized within the cell chamber (~5 min after injection through the airlock). Orange arrows track an individual atypically elongated bacterium during internalization by the cell. Loss of fluorescence is seen (D and E) between 30 and 40 min after binding was initiated. At later time points (G–I), extensive membrane spreading is observed, and yellow arrows indicate the margins. Time marks represent hour and minutes, and the white bar indicates 25 μm. The complete dataset for this figure is represented in a supplemental movie available at http://www.cbi.pitt.edu/movies/leuk.html. This image represents a typical cell observed in experiments from multiple DC preparations.

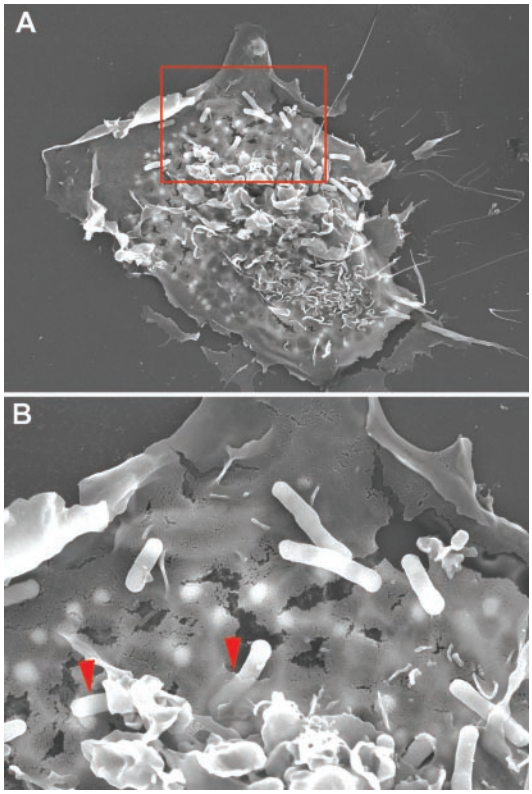

Fig. 4. SEM image of DC following interaction with *E. coli*. Cells were incubated for 2 h with bacteria before washing in phosphate-buffered saline, fixation, and analysis. Arrows indicate bacteria in the process of entering the cell. In this image and many others examined, the thin membrane veils or extensions were particularly susceptible to processing artifacts such as cracking.

were visualized within the cell chamber (~5 min after injection). EGFP-expressing *E. coli* BL21 strain (Novagen, Madison, WI) was injected via the airlock 30 min after beads and images were collected at the same stage positions and intervals. Approximately equal numbers of beads and bacteria were injected. In all images analyzed, beads were observed to flow past cells without triggering membrane ruffling or extension of pseudopods (Fig. 1). Following addition of *E. coli*, DC extended pseudopods and captured bacteria (green) selectively, even as beads (red) flowed past in close proximity to cells. Pseudopod extension and selective capture of bacteria by another cell within the same experiment are shown very clearly in **Figure 2**. These data are also represented in movie format in supplemental data available at the following URL: http://www.cbi.pitt.edu/movies/leuk.html. These results suggest that DC can selectively bind and internalize *E. coli*, perhaps through a receptor-mediated endocytic process that is lacking for the beads. Previous reports demonstrating bead uptake by DC [11, 12] and unpublished studies from our own laboratory generally involved the use of very high-bead concentrations under static conditions or with beads and cells centrifuged together, conditions that would be expected to bring beads into close proximity with the plasma membrane. In contrast, in the current study, particles were allowed to flow past DC, and efficient uptake involved active extension of membrane processes.

To address whether DC responded to bacteria by making more extensive membrane ruffles that could increase the number of bacteria encountered, cells were imaged for longer time periods at higher magnification to optimize visualization of membrane ruffles. **Figure 3** shows such an experiment in which *E. coli* were added as a bolus 5 min before images were collected, and medium was allowed to flow through the chamber for an additional 4 h. More extensive membrane spreading was observed 2–4 h after an initial encounter with *E. coli*, and this continued even in the absence of added bacteria. Membrane spreading was often polarized and directed toward incoming bacteria flowing through the chamber. After binding to veils, which are quite thin, bacteria are retracted toward the center of the cell, where internalization occurs, as seen in Figure 3, and in the associated supplemental movie. Based on

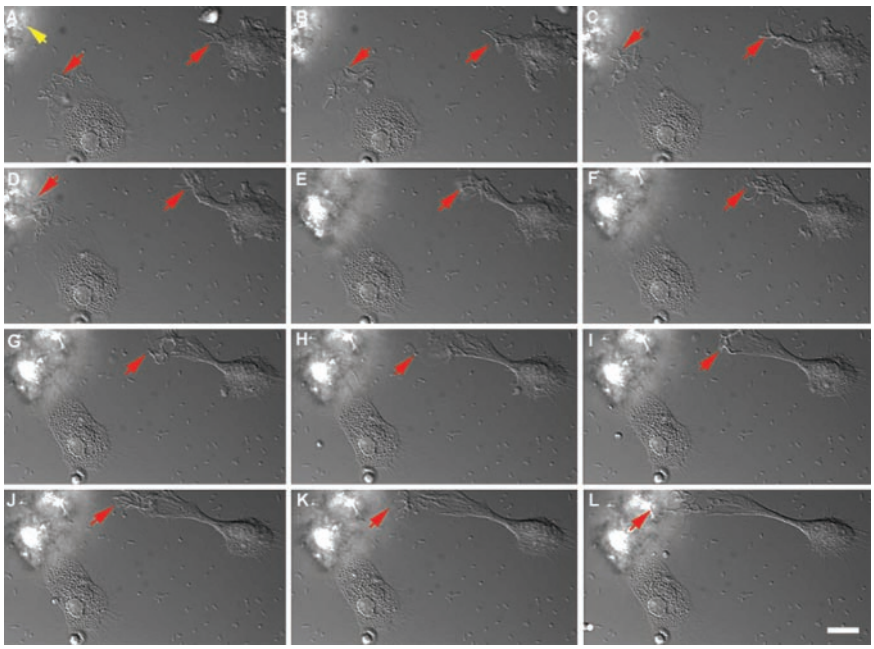

Fig. 5. DC can extend long dendritic processes toward relatively distant objects such as clumps of bacteria. (A) Two relatively quiescent DC (orange arrows), when a large clump of *E. coli* enters the field (yellow arrow) ~45 min after bacteria were injected. In this experiment, nonfluorescent bacteria were used, and individual bacterium can be seen throughout the field. Both DC respond rapidly by extending membrane processes, and the cell on the right provides a particularly striking example of an extension more than 50 μm in length. The 12 individual images were selected from those obtained over a 19-min time-period, indicating how rapidly these cells can respond to stimuli. This type of morphologic change was observed in multiple experiments but is less frequently observed than the membrane spreading seen in Figures 1–3. White bar, 15 μm. The complete dataset for this figure is represented in a supplemental movie available at http://www.cbi.pitt.edu/movies/leuk.html.

the disappearance of fluorescence in the live-cell imaging, we estimate that EGFP is degraded within 20–40 min of bacterial uptake. To directly visualize where DC internalize bacteria, we exposed cells to bacteria and then fixed them before analysis by scanning electron microscopy (SEM). This revealed that bacteria sink into the plasma membrane in the central region of the cell, not in the veils, as seen in **Figure 4**.

In some fields, we observed extension of highly elongated dendritic processes by cells, typically in response to the presence of large clumps of bacteria as seen in **Figure 5** and the associated supplemental movie. This process occurred quite rapidly, and full extension of processes was more than 50 μm in length toward the clump, occurring within 5 min, and was distinct from localized changes such as membrane ruffling and veil extension, seen in response to individual bacteria. This suggests that extension of long dendritic processes requires chemotactic sensing of the stimulus.

In conclusion, our data demonstrate that immature DC derived from human monocytes exhibit diverse responses during encounter with distinct types of particles. One type of response, membrane ruffling and extension of membrane veils, has previously been reported for macrophages during bacterial phagocytosis [13, 14], and a second, elaboration of long dendritic processes, has not. It is likely that distinct signaling programs underlie these events, and it will be important to characterize the underlying processes biochemically to fully understand how DC respond to bacteria and other environmental stimuli.

ACKNOWLEDGMENTS

The authors thank Dr. Andrea Gambotto for providing the EGFP-encoding plasmid. This work was supported by grant CA73743 from NIH (Bethesda, MD).

REFERENCES

1. Lanzavecchia, A. (1996) Mechanisms of antigen uptake for presentation. *Curr. Opin. Immunol.* **8,** 348–354.
2. Albert, M. L., Pearce, S. F., Francisco, L. M., Sauter, B., Roy, P., Silverstein, R. L., Bhardwaj, N. (1998) Immature dendritic cells phagocytose apoptotic cells via αvβ5 and CD36, and cross-present antigens to cytotoxic T lymphocytes. *J. Exp. Med.* **188,** 1359–1368.
3. Kovacsovics-Bankowski, M., Clark, K., Benacerraf, B., Rock, K. L. (1993) Efficient major histocompatibility complex class I presentation of exogenous antigen upon phagocytosis by macrophages. *Proc. Natl. Acad. Sci. USA* **90,** 4942–4946.
4. Villanueva, M. S., Fischer, P., Feen, K., Pamer, E. G. (1994) Efficiency of MHC class I antigen processing: a quantitative analysis. *Immunity* **1,** 479–489.
5. Stubbs, A. C., Martin, K. S., Coeshott, C., Skaates, S. V., Kuritzkes, D. R., Bellgrau, D., Franzusoff, A., Duke, R. C., Wilson, C. C. (2001) Whole recombinant yeast vaccine activates dendritic cells and elicits protective cell-mediated immunity. *Nat. Med.* **7,** 625–629.
6. Higgins, D. E., Shastri, N., Portnoy, D. A. (1999) Delivery of protein to the cytosol of macrophages using *Escherichia coli* K-12. *Mol. Microbiol.* **31,** 1631–1641.
7. Dong, X., Storkus, W. J., Salter, R. D. (1999) Binding and uptake of agalactosyl IgG by mannose receptor on macrophages and dendritic cells. *J. Immunol.* **163,** 5427–5434.
8. Sallusto, F., Cella, M., Danieli, C., Lanzavecchia, A. (1995) Dendritic cells use macropinocytosis and the mannose receptor to concentrate macromolecules in the major histocompatibility complex class II compartment: downregulation by cytokines and bacterial products. *J. Exp. Med.* **182,** 389–400.
9. Romani, N., Gruner, S., Brang, D., Kampgen, E., Lenz, A., Trockenbacher, B., Konwalinka, G., Fritsch, P. O., Steinman, R. M., Schuler, G. (1994) Proliferating dendritic cell progenitors in human blood. *J. Exp. Med.* **180,** 83–93.
10. Romani, N., Kampgen, E., Koch, F., Heufler, C., Schuler, G. (1990) Dendritic cell production of cytokines and responses to cytokines. *Int. Rev. Immunol.* **6,** 151–161.
11. Reece, J. C., Vardaxis, N. J., Marshall, J. A., Crowe, S. M., Cameron, P. U. (2001) Uptake of HIV and latex particles by fresh and cultured dendritic cells and monocytes. *Immunol. Cell Biol.* **79,** 255–263.
12. Fanger, N. A., Wardwell, K., Shen, L., Tedder, T. F., Guyre, P. M. (1996) Type I (CD64) and type II (CD32) Fc γ receptor-mediated phagocytosis by human blood dendritic cells. *J. Immunol.* **157,** 541–548.
13. Alpuche-Aranda, C. M., Racoosin, E. L., Swanson, J. A., Miller, S. I. (1994) Salmonella stimulate macrophage macropinocytosis and persist within spacious phagosomes. *J. Exp. Med.* **179,** 601–608.
14. Rollag, H., Hovig, T. (1984) Phagocytosis of non-opsonized *Escherichia coli* by mouse peritoneal macrophages. An electron microscopic study. *Zentralbl. Bakteriol. Mikrobiol. Hyg. [A]* **257,** 93–107.